

# Quantum correlations of confined exciton-polaritons

Aymeric Delteil<sup>1\*</sup>, Thomas Fink<sup>1\*</sup>, Anne Schade<sup>2</sup>, Sven

Höfling<sup>2,3</sup>, Christian Schneider<sup>2</sup> and Ataç İmamoğlu<sup>1</sup>

<sup>1</sup> *Institute of Quantum Electronics, ETH Zurich, 8093 Zurich, Switzerland.*

<sup>2</sup> *Technische Physik, Universität Würzburg, Würzburg, Germany.*

<sup>3</sup> *SUPA, School of Physics and Astronomy,*

*University of St Andrews, St Andrews, UK.*

*\* These authors contributed equally to this work.*

Cavity-polaritons in semiconductor microstructures have emerged as a promising system for exploring nonequilibrium dynamics of many-body systems [1]. Key advances in this field, including the observation of polariton condensation [2], superfluidity [3], realization of topological photonic bands [4], and dissipative phase transitions [5–7], generically allow for a description based on a mean-field Gross-Pitaevskii formalism. While observation of polariton intensity squeezing [8, 9] and decoherence of a polarization entangled photon pair by a polariton condensate [10] provide counterexamples, quantum effects in these experiments show up at high polariton occupancy. Going beyond into the regime of strongly correlated polaritons requires the observation of a photon blockade effect [11, 12] where interactions are strong enough to suppress double occupancy of a photonic lattice site. Here, we report the observation of quantum correlations between polaritons in a fiber cavity which spatially confines polaritons into an area of  $3 \mu\text{m}^2$ . Photon correlation measurements show that careful tuning of the coupled system allows for a modest photon blockade effect as evidenced by a reduction of simultaneous two-polariton generation probability by 5 %. Concurrently, our experiments provide an unequivocal measurement of the polariton interaction strength, thereby resolving the controversy stemming from recent experimental reports [13]. Our findings constitute a first essential step towards the realization of strongly interacting photonic systems.

Photon blockade can be described as strong conditional modification of optical properties of a medium by a single photonic excitation. The early demonstrations of photon blockade were

based on the realization of the Jaynes-Cummings model consisting of a single anharmonic quantum emitter strongly coupled to a cavity mode. The requisite optical nonlinearity in this case originates from the impossibility of double excitation of the anharmonic emitter and consequently of the cavity-emitter system under resonant excitation. In the opposite limit of a collective excitation of a large number of two-level emitters coupled to a cavity mode, photon blockade can only be observed if there is strong interaction between optically excited collective states. This for example is manifestly the case if the incident field creates a collective excitation to a Rydberg state with large van der Waals interactions [14, 15]. In condensed matter, an analogous situation can be obtained using quantum well (QW) excitons nonperturbatively coupled to a cavity mode, leading to the formation of hybrid light-matter eigenstates, termed polaritons. In this system, exciton-exciton interactions ensure that the polariton spectrum is anharmonic, provided that polaritons are confined to maximize their in-plane spatial overlap. If the interaction-induced energy shift is larger than the polariton linewidth, the system exhibits polariton blockade [12]. A convenient verification of the blockade phenomenon is provided by photon antibunching – a vanishing photon correlation function  $g^{(2)}(\tau)$  for delays  $\tau$  smaller than the polariton lifetime. Even in the limit where the nonlinearity is smaller than the linewidth, finite photon antibunching can be observed provided that the laser is detuned from the polariton center frequency. Such an observation confirms a first-order modification of the cavity transmission conditioned on the excitation of a single polariton [16].

To demonstrate quantum correlations of confined polaritons, we measure  $g^{(2)}(\tau)$  using photons transmitted from a resonantly driven zero-dimensional cavity that is strongly coupled to the excitonic transition of a QW [7, 17]. Figure 1a depicts the experimental set-up based on a semi-integrated fiber cavity whose length is tunable *in situ* using a piezo-based nanopositioner. The concave surface of the fiber leads to lateral confinement with a mode waist of  $w_0 = 1.0 \mu\text{m}$ . A single InGaAs QW is placed at an antinode of the fundamental  $\text{TEM}_{00}$  mode (see Methods). When scanning the cavity mode energy across the exciton resonance, we observe a large Rabi splitting of  $E_R = 3.5 \text{ meV}$  between the two polariton eigenmodes, signaling the strong coupling regime (Fig. 1b). Focusing exclusively on the lower polariton (LP) mode and neglecting the role of the far detuned upper polariton branch, the Hamiltonian describing the system in the rotating basis under resonant drive reads:

$$H = (\hbar\omega_L - E_{\text{LP}})\hat{p}^\dagger\hat{p} + \frac{U_{\text{pp}}}{2}\hat{p}^\dagger\hat{p}^\dagger\hat{p}\hat{p} + \hbar F^*\hat{p}^\dagger + \hbar F\hat{p} \quad (1)$$

where  $\hat{p}$  denotes the lower polariton annihilation operator,  $\omega_L$  the excitation laser frequency,  $E_{LP}$  the LP energy,  $F$  the drive strength, and  $U_{pp}$  the polariton-polariton interaction strength. The polariton annihilation operator  $\hat{p}$  can be decomposed into its exciton and photon components as  $\hat{p} = c_p \hat{a} + c_x \hat{x}$ , where  $\hat{a}$  ( $\hat{x}$ ) denotes the annihilation operator associated with the cavity mode (QW exciton). The corresponding Hopfield coefficients  $c_p$  and  $c_x$ , satisfying  $|c_p|^2 + |c_x|^2 = 1$ , depend on the cavity-exciton detuning and therefore can be adjusted by changing the cavity length.

In the limit of a small nonlinearity, the maximum degree of antibunching  $A \triangleq \max(1 - g^2(0))$  is approximately given by the ratio between the polariton-polariton interaction energy and the linewidth  $\Gamma_p$ :  $A \approx U_{pp}/\Gamma_p = U_{xx}|c_x|^4/\Gamma_p$  where  $U_{xx}$  is the exciton-exciton interaction energy (see Supplementary Information). Thus, the maximum antibunching is the result of an interplay between polariton linewidth and exciton content. In the following we identify the optimal system parameters allowing the observation of blockade by characterizing the dependence of the lower polariton linewidth and maximum transmission on the cavity mode energy. We perform laser scans of the transmission while varying the cavity length (Fig. 2a), from which we extract the linewidth and maximum transmission. Figure 2b plots the cavity linewidth and transmission as a function of the LP energy: as we increase  $E_{LP}$  by reducing the cavity length, the linewidth experiences a moderate increase up to  $E_{LP} \approx 1.468$  eV. For higher  $E_{LP}$ , the linewidth increases sharply while the corresponding maximum transmission drops.

In order to identify the contributions to the polariton linewidth, we model the optical response of our cavity with an input-output formalism [18] where we use experimentally measured parameters: the Rabi splitting  $E_R = 3.5$  meV, the disorder dominated (bare) exciton linewidth  $h\Delta\nu_x = 0.5$  meV measured outside the cavity, and the bare cavity linewidth  $\kappa = 28$   $\mu$ eV. The only free parameter in our model is a Markovian exciton decay rate  $\gamma_x$ . We obtain the best agreement with experimental data for  $\gamma_x = 40$   $\mu$ eV (see Supplementary Information). Although the physical process associated with  $\gamma_x$  is unclear, we tentatively attribute this decay channel to disorder mediated coupling of the confined LP mode to guided modes of the planar structure. A better understanding of this decay channel would be beneficial since its elimination could lead to a sizable increase in the degree of antibunching. On the other hand, the coupling to localized exciton states has only little effect on the polariton linewidth as long as we maintain negligible overlap between the LP mode and the inhomogeneously broadened bare exciton spectrum [19].

This characterization allows to identify the optimal cavity-exciton detuning  $\delta_{c-x}$  for maximizing

quantum correlations between polaritons, or equivalently,  $A \propto |c_x|^4/\Gamma_p$ . Figure 2c shows this ratio calculated for both our data and our model, as a function of the exciton content. We deduce from this plot that the exciton content at which we expect the highest degree of antibunching is about  $|c_x|^2 \sim 0.6$ , yielding a polariton lifetime of  $\tau_{LP} = \hbar/\Gamma_p \approx 11$  ps. In the following we use the corresponding optimal value of  $\delta_{c-x}$ .

Since  $\tau_{LP}$  is shorter than the time resolution of single-photon detectors, we employ a pulsed excitation where the pulse width  $\tau_L$  of the laser pulses is a factor of  $\approx 3$  longer than  $\tau_{LP}$  [20]. The only requirement on detector bandwidth in this case is that it exceeds the laser repetition rate of 80 MHz. This approach allows us to implement a red-detuned excitation where all laser frequency components satisfy  $\hbar\omega_L < E_{LP}$ , thereby ensuring that  $A$  is maximal for repulsive interactions ( $U_{pp} > 0$ ). On the other hand, we cannot rule out multiple excitations during the timescale given by  $\tau_L$ , which reduces the magnitude of the measured  $A$ .

Photons emitted from the cavity are collected in a single mode fiber and transferred to a Hanbury Brown and Twiss setup where the coincidences are recorded. The upper (lower) panel of Fig. 3a shows the histogram obtained at  $\Delta = \hbar\omega_{L0} - E_{LP} = -0.75\Gamma_p$  ( $+0.5\Gamma_p$ ), where  $\omega_{L0}$  denotes the center frequency of the laser pulse. In the red-detuned case ( $\Delta < 0$ ), we observe that the number of coincidences corresponding to a period difference of 0 is lower than the average value of the other periods, while the opposite is true for the blue-detuned case. We deduce from each histogram the corresponding integrated second order correlation  $\tilde{g}^2[0]$  (see Methods).

Figure 3b shows  $\tilde{g}^2[0]$  as a function of the laser detuning, obtained by repeating such measurements while scanning the laser energy. We observe a minimum of  $\tilde{g}^2[0] = 0.95 \pm 0.02$  for  $\Delta = -0.75\Gamma_p$ . The value for  $\Delta = 0$  lies above unity; we tentatively attribute this bunching signal to feeding of the LP resonance by a thermal localized exciton bath. Repeating these measurement for different incident laser powers allows us to obtain the contour plot in Fig. 3c where we show the value of  $\tilde{g}^2[0]$  as a function of the laser detuning and power. This plot is constructed from 63 data points measured with power- and detuning-dependent integration times, varying from 0.5 h to 8.5 h per point, for a total measurement time of 82 h. It is evident that photon antibunching is present for small red detunings up to a power of  $\sim 20$  nW and vanishes at higher excitation power.

The determination of  $U_{xx}$  has been previously carried out using the polariton density dependent blue shift of the LP resonance. Such measurements, however, are inherently inaccurate due to the difficulty in estimating the actual exciton population which has contributions not only from

polaritons but also from long-lived localized excitons. The latter are generated even under resonant excitation, as evidenced by the bunching signal we observe for  $\Delta = 0$ . On the other hand, the minimum value of  $\tilde{g}^{(2)}$  directly gives a lower bound on  $U_{xx}$  without requiring an estimation of the exciton population (see Supplementary Material). From our measurements we estimate  $U_{pp} = 13 \pm 6 \mu\text{eV}$ , yielding  $U_{xx} = 40 \mu\text{eV}\mu\text{m}^2$ , in agreement with what has been estimated by several groups [6, 20–22].

Our results demonstrate that the cavity-exciton response to a drive field can be sizably modified by the presence of a single polariton. Together with Ref. [20], our observations demonstrate quantum behavior of polaritons that cannot be captured by mean-field methods. While the degree of quantum correlations we report are modest, further enhancement of the degree of antibunching could be reached by decreasing the polariton linewidth by employing higher quality QW samples with reduced disorder. Alternatively,  $U_{xx}$  could be enhanced by using dipolar polaritons in coupled QWs [23] embedded in microcavities, or polaron-polaritons in the fractional quantum Hall regime [24].

## METHODS

**Experimental set-up.** The experiments are based on an open cavity structure where the top mirror is a concave distributed Bragg reflector (DBR) mirror deposited on a fiber. A dimple with a radius of curvature of  $13.9 \mu\text{m}$  is created on the center of the fiber facet using  $\text{CO}_2$  laser ablation. The bottom (output) mirror is integrated in the sample and consists of an AlAs/GaAs DBR grown by molecular beam epitaxy. The InGaAs QW is grown on top of this latter DBR during the same growth process. The light transmitted through the cavity is collimated from the back of the sample and collected into a fiber that guides it to a Hanbury Brown and Twiss set-up.

**Photon correlation measurements.** We drive the cavity using a Ti:Sapphire picosecond laser with 80 MHz repetition rate. We prolong the pulses using a monochromator of bandwidth  $20 \mu\text{eV}$ . The center wavelength of the laser pulses is set by controlling the grating angle. The transmitted photons are detected by two fiber-based commercial avalanche photodiodes of quantum efficiency 45 % and timing jitter 300 ps, and the detection events are recorded using a time-tagged single photon counter. The photon records are binned according to the number of laser periods  $\Delta T$  separating their detection. The integrated  $\tilde{g}^{(2)}[0]$  is defined as the ratio between the coincidence

number with  $\Delta T = 0$  to the average of the coincidence number having  $\Delta T \neq 0$  calculated from 20 consecutive periods around the zero delay.

- 
- [1] Carusotto, I. & Ciuti, C. Quantum fluids of light. *Rev. Mod. Phys.* **85**, 299 (2013).
  - [2] Kasprzak *et al.* Bose-Einstein condensation of exciton polaritons. *Nature* **443**, 409-414 (2006).
  - [3] Amo, A. *et al.* Superfluidity of polaritons in semiconductor microcavities. *Nat. Phys.* **5**, 805-808 (2009).
  - [4] Lasing in topological edge states of a one-dimensional lattice. *Nat. Photon.* **11**, 651-656 (2017).
  - [5] Ohadi, H. *et al.* Spin order and phase transitions in chains of polariton condensates. *Phys. Rev. Lett.* **119**, 067401 (2017).
  - [6] Rodriguez, S.R.K. *et al.* Probing a dissipative phase transition via dynamical optical hysteresis. *Phys. Rev. Lett.* **118**, 247402 (2017).
  - [7] Fink, T., Schade, A., Höfling, S., Schneider, C. & Imamoglu, A. Signatures of a dissipative phase transition in photon correlation measurements. *Nat. Phys.* **14**, 365-369 (2018).
  - [8] Karr, J. Ph., Baas, A., Houdre, R. & Giacobino, E. Squeezing in semiconductor microcavities in the strong coupling regime. *Phys. Rev. A* **69**, 031802(R) (2004).
  - [9] Boulier, T., Bamba, M., Amo, A., Adrados, C., Lemaître, A., Galopin, E., Sagnes, I., Bloch, J., Ciuti, C., Giacobino, E. & Bramati, A. Polariton-generated intensity squeezing in semiconductor micropillars. *Nat. Commun.* **5**, 3260 (2014).
  - [10] Cuevas, A. *et al.* First observation of the quantized exciton-polariton field and effect of interactions on a single polariton. *Sci. Adv.* **4**, eaao6814 (2018).
  - [11] Imamoglu, A., Schmidt, H., Woods, G. & Deutsch, M. Phys. Rev. Lett. Strongly interacting photons in a nonlinear cavity. *Phys. Rev. Lett.* **79**, 1467 (1997).
  - [12] Verger, A., Ciuti, C. & Carusotto, I. Polariton quantum blockade in a photonic dot. *Phys. Rev. B* **73**, 193306 (2006).
  - [13] Sun, Y. *et al.* Direct measurement of polariton-polariton interaction strength. *Nat. Phys.* **13**, 870-875 (2017).
  - [14] Cubel Liebisch, T., Reinhard, A., Berman, P. R. & Raithel, G. Atom Counting Statistics in Ensembles of Interacting Rydberg Atoms. *Phys. Rev. Lett.* **95**, 253002 (2005).
  - [15] Urban, E. *et al.* Observation of Rydberg blockade between two atoms. *Nat. Phys.* **5**, 110-114 (2009).
  - [16] Ferretti *et al.* Single-photon nonlinear optics with Kerr-type nanostructured materials. *Phys. Rev. B* **85**, 033303 (2012).
  - [17] Besga, B. *et al.* Polariton boxes in a tunable fiber cavity. *Phys. Rev. Appl.* **3**, 014008 (2015).
  - [18] Diniz, I., Portolan, S., Ferreira, R., Gérard, J.M., Bertet, P. & Auffèves, A. Strongly coupling a cavity

- to inhomogeneous ensembles of emitters: Potential for long-lived solid-state quantum memories. *Phys. Rev. A* **84**, 063810 (2011).
- [19] Houdré, R., Stanley, R.P. & Illegems, M. Vacuum-field Rabi splitting in the presence of inhomogeneous broadening: Resolution of a homogeneous linewidth in an inhomogeneously broadened system. *Phys. Rev. A* **53**, 2711 (1996).
- [20] Muñoz-Matutano, G. *et al.* Quantum-correlated photons from semiconductor cavity polaritons. arXiv:1712.05551 (2017).
- [21] Ferrier, L. *et al.* Interactions in confined polariton condensates. *Phys. Rev. Lett.* **106**, 126401 (2011).
- [22] Rodriguez, S.R.K. *et al.* Interaction-induced hopping phase in driven-dissipative coupled photonic micro-cavities. *Nat. Commun.* **7**, 11887 (2016).
- [23] Togan, E., Lim, H.T., Faelt, S., Wegscheider, W. & Imamoglu, A. Strong interactions between dipolar polaritons. arXiv:1804.04975 (2018).
- [24] Ravets, S. *et al.* Polaron polaritons in the integer and fractional quantum Hall regimes. *Phys. Rev. Lett.* **120**, 057401 (2018).

**Supplementary Information** is linked to the online version of the paper at [www.nature.com/nature](http://www.nature.com/nature).

**Acknowledgments** This work was supported by the Swiss National Science Foundation (SNSF) through a DACH project 200021E-158569-1, SNSF National Centre of Competence in Research - Quantum Science and Technology (NCCR QSIT) and an ERC Advanced investigator grant (POLTDES). The Würzburg Group acknowledges support by the state of Bavaria, and the DFG within the project SCHN1376-3.1

**Author Contributions** A.D., T.F. and A.I. supervised the project. T.F. designed the experiment. A.D. and T.F. carried out the measurements. A.S., C.S., and S.H. grew the sample. A.D. and A.I. wrote the manuscript.

**Author Information** Reprints and permissions information is available at [www.nature.com/reprints](http://www.nature.com/reprints). The authors declare that they have no competing financial interests. Correspondence and requests for materials should be addressed to [imamoglu@phys.ethz.ch](mailto:imamoglu@phys.ethz.ch).

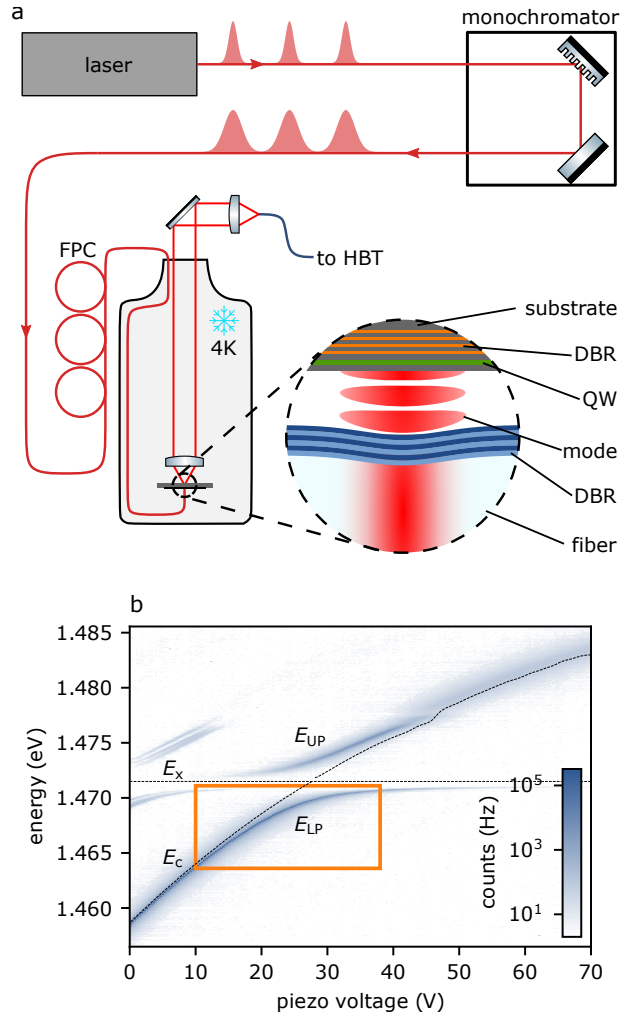


Figure 1: **Experimental set-up for cavity-polaritons.** (a) A fiber cavity is driven by either a cw laser or ps laser pulses whose pulsewidth is prolonged by a monochromator. The polarization set by fiber polarization controllers (FPC) is chosen to match the lowest linearly polarized cavity mode. The transmitted light is collected in a fiber and guided to a Hanbury Brown and Twiss (HBT) setup where photon statistics are measured. Zoom-in: Structure of the semi-integrated cavity. (b) White light transmission spectra as a function of the piezo voltage controlling the cavity length, revealing a Rabi splitting of 3.5 meV. The orange box indicates the region of interest for the present work.



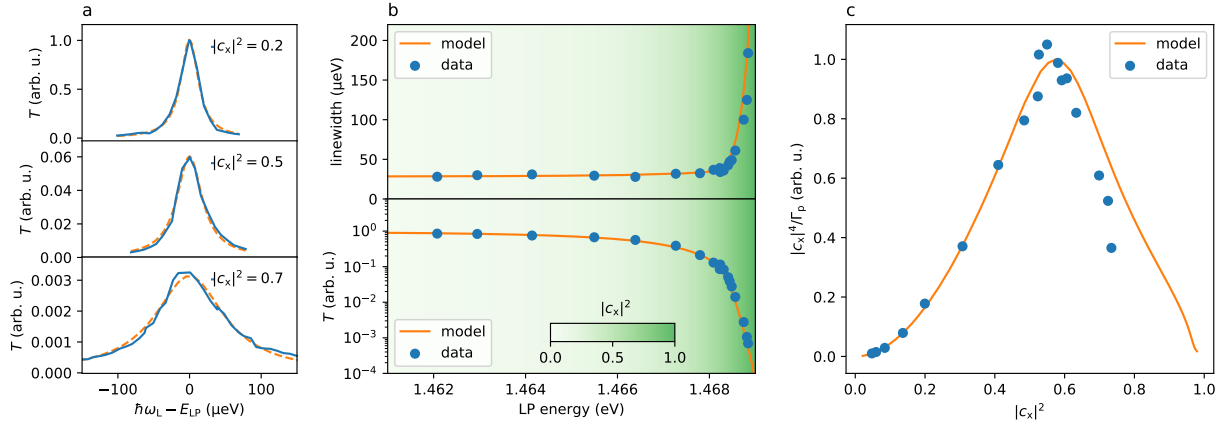


Figure 2: **Optimization of polariton parameters.** (a) Transmission spectra measured at three different cavity-exciton detunings (blue line) depicted together with the Lorentzian fit to the data (orange dashed line). (b) Upper panel: polariton linewidth  $\Gamma_P$  extracted from the transmission measurements, as a function of the LP energy (blue dots) and linewidth calculated from the simulation (orange curve). Lower panel: Maximum measured polariton transmission as a function of the LP energy (blue dots) and simulated maximum cavity transmission (orange curve). The background color plot indicates the Hopfield coefficient corresponding to the lower polariton energy. (c) The ratio  $|c_x|^4 / \Gamma_P$  which quantifies the maximum attainable quantum correlations as a function of the exciton content  $|c_x|^2$  of the lower polariton (blue dots). The calculated ratio  $|c_x|^4 / \Gamma_P$  (orange curve).

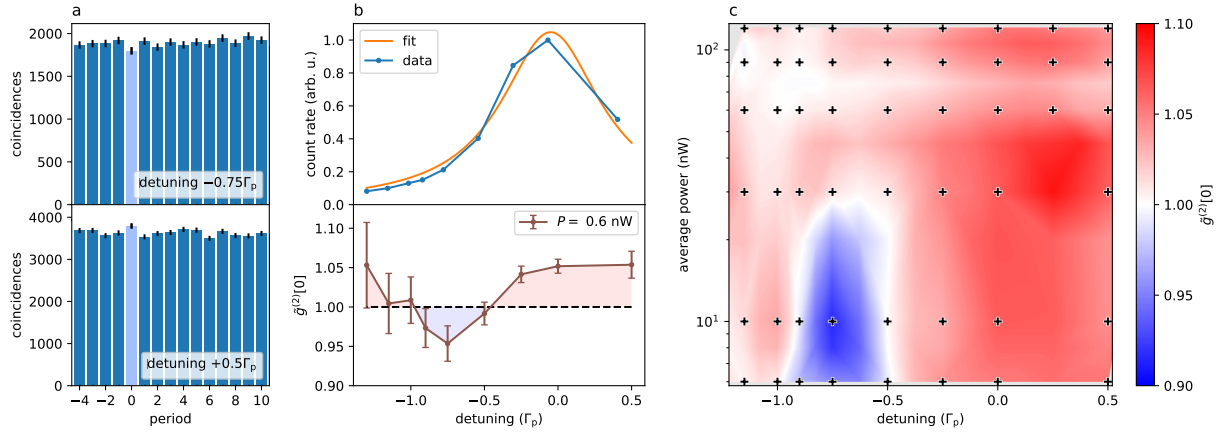


Figure 3: **Quantum correlations between polaritons.** (a) Upper panel: Coincidence number in pulsed regime as a function of the period difference between the two detected photons, at a detuning of  $\Delta = -0.75\Gamma_p$ . Lower panel: Same as the upper panel, but at a detuning of  $\Delta = +0.5\Gamma_p$ . (b) Upper panel: Photon rate as a function of the laser detuning (blue curve). Lorentzian fit to the data (orange curve). Lower panel: Integrated  $\tilde{g}^2[0]$  as a function of the laser detuning. The dashed black line indicates the value for uncorrelated photons. (c) Integrated  $\tilde{g}^2[0]$  as a function of the laser detuning and power. The black crosses indicate the detuning and power at which the measurements are carried out. The blue areas are below the classical limit given by  $\tilde{g}^2[0] \geq 1$ . The  $\tilde{g}^2[0]$  dependence on detuning shown in (b) corresponds to the lowest depicted power.